CENTER FOR CONNECTED AND AUTOMATED TRANSPORTATION

Final Report #8
December 2022

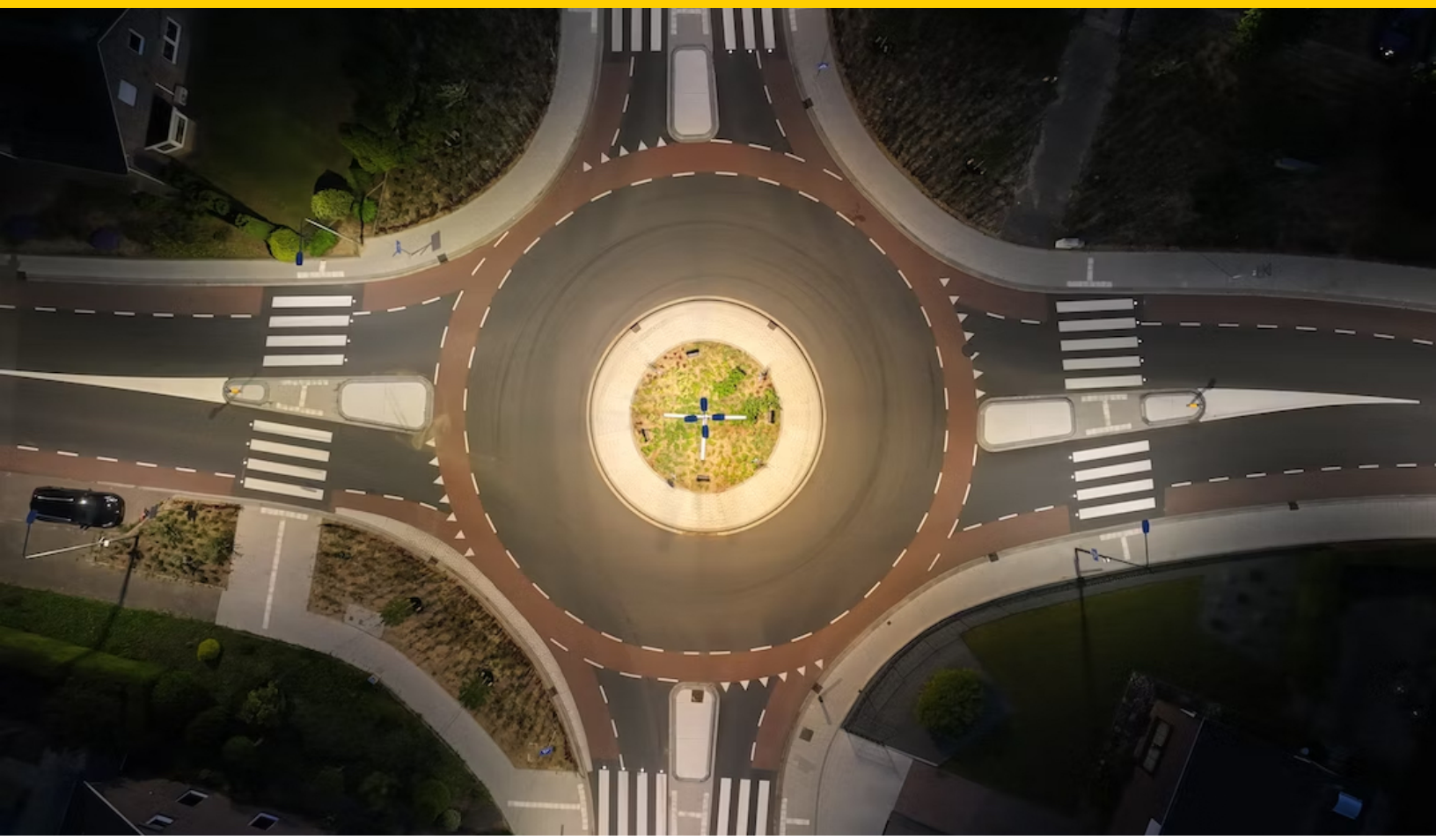

Adapting Land Use and Infrastructure for Automated Driving

Chaojie Wang
Einat Tenenboim
Srinivas Peeta

PURDUE UNIVERSITY®

CENTER FOR CONNECTED AND AUTOMATED TRANSPORTATION

Report No. 8
Report Date: December 2022
Project Start Date: 1/1/2018
Project End Date: 12/31/2022

Adapting Land Use and Infrastructure for Automated Driving

Chaojie Wang
Graduate Researcher
Georgia Institute of Technology

Einat Tenenboim
Postdoctoral Fellow
Georgia Institute of Technology

Srinivas Peeta
Frederick R. Dickerson Chair & Professor
Georgia Institute of Technology

UMTRI | The University of Akron | Illinois Center for Transportation | Purdue University | Washtenaw Community College | Central State University

ACKNOWLEDGEMENTS AND DISCLAIMER

Funding for this research was provided by the Center for Connected and Automated Transportation under Grant No. 69A3551747105 of the U.S. Department of Transportation, Office of the Assistant Secretary for Research and Technology (OST-R), University Transportation Centers Program. The work was carried out by researchers at the Georgia Institute of Technology through a subcontract with Purdue University. The contents of this report reflect the views of the authors, who are responsible for the facts and the accuracy of the information presented herein. This document is disseminated under the sponsorship of the Department of Transportation, University Transportation Centers Program, in the interest of information exchange. The U.S. Government assumes no liability for the contents or use thereof.

Suggested APA Format Citation:

Wang, C., Tenenboim, E., Peeta, S. (2022). Adapting Land Use and Infrastructure for Automated Driving, CCAT Report #8, Center for Connected and Automated Transportation, Purdue University, W. Lafayette, IN.

Contact Information

Samuel Labi
Purdue University
3000 Kent Ave., West Lafayette, IN
Phone: (765) 494-5926
Email: labi@purdue.edu

Srinivas Peeta
Georgia Institute of Technology
3000 Kent Ave, West Lafayette, IN
Phone: (404) 894-2300
Email: peeta@gatech.edu

CCAT
University of Michigan Transportation Research Institute
2901 Baxter Road
Ann Arbor, MI 48152

uumtri-ccat@umich.edu
(734) 763-2498
www.ccat.umtri.umich.edu

Technical Report Documentation Page

1. Report No. CCAT Report #8	**2. Government Accession No.** N/A	**3. Recipient's Catalog No.** N/A
4. Title and Subtitle Adapting land use and infrastructure for automated driving		**5. Report Date** December 2022
		6. Performing Organization Code N/A
7. Author(s) Chaojie Wang, Einat Tenenboim, Srinivas Peeta		**8. Performing Organization Report No.** N/A
9. Performing Organization Name and Address Center for Connected and Automated Transportation Purdue University, 550 Stadium Mall Drive, W. Lafayette, IN 47907; and University of Michigan Ann Arbor, 2901 Baxter Road, Ann Arbor, MI 48109		**10. Work Unit No.**
		11. Contract or Grant No. Contract No. 69A3551747105
12. Sponsoring Agency Name and Address U.S. Department of Transportation Office of the Assistant Secretary for Research and Technology 1200 New Jersey Avenue, SE, Washington, DC 20590		**13. Type of Report, Period Covered** Final Report, 1/1/2018 - 12/31/2022
		14. Sponsoring Agency Code OST-R

15. Supplementary Notes
Conducted under the U.S. DOT Office of the Assistant Secretary for Research and Technology's (OST-R) University Transportation Centers (UTC) program.

16. Abstract
Intersections in the urban network are potential sources of traffic flow inefficiency. Existing intersection control mostly adopts the "cross" flow pattern model, while the use of the roundabout circular flow pattern is rather sparse. Connected and autonomous vehicle (CAV) technologies can enable roundabouts to better compete with traditional intersection designs in terms of performance. This study proposes a roundabout control strategy for CAVs to enhance intersection performance while ensuring vehicle safety. A hierarchical framework is developed to decouple the flow-level performance objective and vehicle-level safety constraints to achieve computational tractability for real-time applications. It entails developing a roundabout flow control model to optimize merge-in flows, a merge-in decision model to generate vehicle passing sequence from the optimal flows, and a virtual platoon control model to achieve safe and stable vehicle operations in a circular roundabout platoon. The performance of the proposed roundabout control strategy is illustrated through numerical studies and compared to existing intersection control methods. Its stability and safety characteristics are also demonstrated.

17. Key Words Roundabout, Optimal control, Connected and Autonomous vehicle	**18. Distribution Statement** No restrictions.		
19. Security Classif. (of this report) Unclassified	**20. Security Classif. (of this page)** Unclassified	**21. No. of Pages** 29 pages	**22. Price** Leave blank – not used

Form DOT F 1700.7 (8-72) Reproduction of completed page authorized

CCAT CENTER FOR CONNECTED AND AUTOMATED TRANSPORTATION

TABLE OF CONTENTS

LIST OF FIGURES

LIST OF TABLES

1. INTRODUCTION

Traffic smoothness is a description of the consistency and invariance of traffic flow. A common symptom of unsmooth traffic is traffic oscillations, which is the "stop-and-go" or "slow-and-fast" flow pattern (Wang et al. 2020). Traffic oscillations can result in traffic congestion, thus affecting traffic capacity, reducing traffic safety, and increasing energy consumption. Compared to traffic flow on freeways, urban network traffic has lesser smoothness due to the presence of intersections. The intersection is an essential component of urban road networks. Compared to other road facilities, traffic flow conflicts are more complex at intersections due to the number of different flow directions (Levin & Rey 2017). Therefore, the efficiency and capacity of an intersection are critical factors for measuring urban transportation system performance. In general, intersections are stop-controlled or signal-controlled. Stop-controlled intersections do not allow multiple vehicles to use the intersection at the same time to ensure safety, which can be inefficient in high-demand cases. Traffic signals separate conflicting traffic flows into different signal phases to enhance the intersection safety. However, the variance and uncertainty in demand decrease the efficiency of signalized intersections. Intersection signal optimization methods, such as (Li, Elefteriadou & Ranka 2014; Eom & Kim 2020), focus on optimizing the phase lengths to the incoming demands adaptively to reduce inefficient phase time and enhance the overall throughput of the intersection. However, due to the existence of the red phase, traffic has to stop at intersections, leading to limited smoothness.

Compared to signalized intersections, a roundabout has smoother traffic flow characteristics. Roundabouts are circular intersections where road traffic only flows in one direction around a central island. Vehicles only yield to the traffic rather than stop entirely at entry points of the roundabout. Therefore, roundabouts can enhance the smoothness of the intersection. (Retting et al. 2006) showed that there is an 89 percent reduction in delays and a 56 percent reduction in vehicle stops after the conversion from signalized intersections to roundabouts. Also, roundabouts can improve traffic safety. On the one hand, vehicles will not speed up to try to beat a traffic light because there is no incentive that vehicles can skip a long red phase if they do so. On the other hand, the one-way traffic in the roundabout reduces the possibility of severe T-bone and head-on collisions. (Retting et al. 2006) found a 72-80 percent reduction in injury crashes and a 35-47 percent reduction in all crashes in studies of intersections converted from traffic signals to roundabouts. This is because there are only eight conflicting points in a typical four-approach roundabout (without any crossing conflicting points), while a four-approach signalized intersection has 32 conflicting points (16 of them are crossing conflicting points). Compared to merging and diverging conflicting points, crossing conflicting points can entail a higher likelihood of severe accidents because vehicles have higher relative speeds. However, since traffic flows from different directions are not as clearly separated as in signalized intersections, there are more merging and diverging behaviors in roundabouts, which can be challenging for human drivers. To ensure safety, drivers are required to operate vehicles at low speeds when passing through a roundabout. Further, signalized intersections can adjust the phase lengths of flows from different directions to achieve better system performance, while roundabouts follow the first-come-first-serve rule more strictly as they lack holistic control schemes. In summary, the lack of precision in human drivers' driving behavior can weaken roundabouts' safety advantage, while the

oversimplified cooperation rules compared to adaptive traffic signal control scheme can limit the system performance and the application of roundabouts in high-demand situations.

Advances in communication and automation technologies have led to the development of connected and autonomous vehicles (CAVs), which can enable accurate vehicle operations and comprehensive cooperation through vehicle-to-vehicle (V2V) communications. CAVs can address the aforementioned limitations of roundabouts in the context of human-driven vehicles and thereby illustrate the advantages of roundabouts over signalized intersections. Existing studies have shown that CAVs are able to enhance system performance with safety guarantees by incorporating additional real-time information collected using V2V communications into comprehensive control schemes (Eisenman et al. 2004; Nie et al. 2016). In this context, cooperative adaptive cruise control (CACC) could be leveraged to ensure CAVs' safety while allowing them to pass through smaller-radius roundabouts at higher speeds. The connectivity ability further enables holistic cooperative control strategies to enhance system performance. Several studies, such as (Malikopoulos, Cassandras & Zhang 2018; Mirheli et al. 2019), have developed such control strategies for traditional intersection geometries without using traffic signals, which are labeled as signal-free intersection control strategies, to reduce traffic oscillations caused by signalized intersections and enhance smoothness. However, the "cross" flow pattern within the intersection remains the same as in signalized intersections, thereby retaining the safety issues caused by crossing conflicting points. For safety reasons, more constraints are incorporated in signal-free intersection control models, which further constrains the enhancement of system performance under CAV technologies.

While roundabouts can potentially enable better performance in a CAV environment compared to signal-free intersections, few efforts have focused on developing roundabout control strategies. (Rastelli & Peñas 2015) proposed a fuzzy logic steering control for autonomous vehicles in roundabouts. (González, Pérez & Milanés 2017) developed a parameter-based path generation method for autonomous vehicles in roundabouts. However, these studies focus on the control strategy for a single-vehicle scenario. Other studies (Banjanovic-Mehmedovic et al. 2016; Tian et al. 2018) proposed game-theoretic-based decision-making methods for a two-vehicle scenario in a roundabout. Hence, existing studies address the control problem for specific scenarios and cannot be generalized to high-demand intersections. Moreover, they mainly address safety considerations. However, demand is typically higher at intersections in urban networks, which entails the need for system performance (i.e., smoothness, total delays, and throughput) analysis for intersection control strategies. This motivates the need for a systematic approach to leverage the advantages of roundabouts in the CAV context.

This study proposes a cooperative roundabout control strategy for CAVs to exploit the advantages of roundabout design to promote performance efficiency of roundabouts while ensuring vehicle safety. As shown in Figure 1, the proposed model is a hierarchical framework that consists of a roundabout flow control model, a merge-in decision model, and a within-roundabout virtual platoon control model. The time horizon of interest is divided into equal time intervals within which the incoming demands of the roundabout are assumed constant. During each time interval τ, the proposed roundabout flow control model solves for the optimal desired merge-in flows (which are the flows merging into the circular flow within the roundabout) to reduce the total

estimated waiting time in queues in the current time interval to enhance system performance. Then, the vehicle merge-in control model performs a probabilistic merge-in decision control to achieve the optimal merge-in flows and generate the vehicle passing sequence (vehicles' positions in the virtual platoon) at the same time. Finally, a CACC-based in-roundabout virtual platoon control model is proposed to keep the circular platoon cruising at the desired angular speed in a stable manner while each vehicle maintains a safe distance with the preceding and following vehicles.

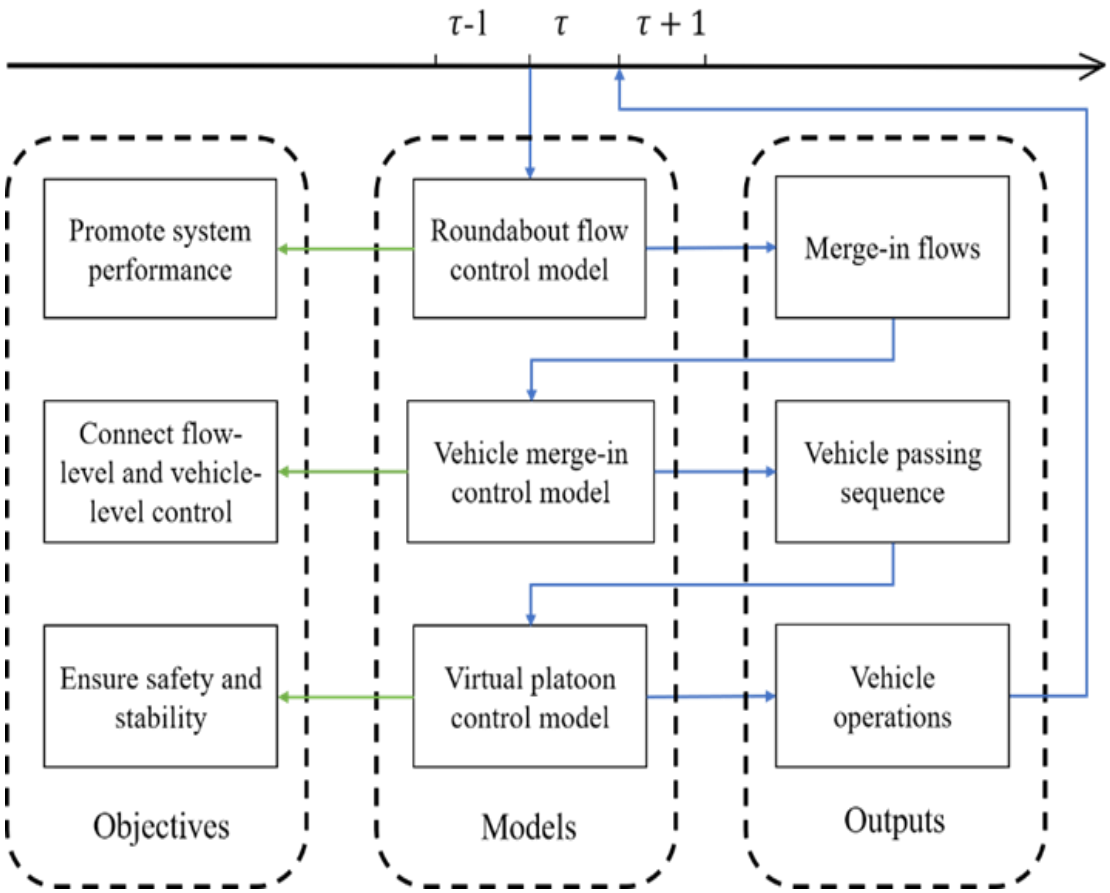

Figure 1.1: Conceptual structure of the roundabout control strategy

The rest of the report is organized as follows. The next chapter presents the three components of the proposed roundabout control strategy. Numerical studies on the effectiveness of the roundabout flow control and virtual platoon control are discussed in subsequent chapters. The final chapter concludes the report by summarizing contributions and identifying potential future directions.

2. METHODOLOGY

2.1 Roundabout flow control

Consider a typical roundabout shown in Figure 2.1, which has four approaches indexed by $i = 1, 2, 3, 4$. The incoming flows on the four approaches are denoted by Q_i, assumed constant during each time period τ, and known at the beginning. The queue length on approach i, $l_i(t)$, is a state variable of t. In each time period, t starts from 0 and ends at $\Delta\tau$ (the time period length). Merge-in flows, $q_i(t)$, are control inputs, which represent the flows merging into the circular flow within the roundabout from approach i. The queue length dynamics can be described as

$$\frac{dl_i(t)}{dt} = Q_i - q_i(t), \forall i = 1, 2, 3, 4. \tag{2.1}$$

Apart from the non-negative constraint, it is also reasonable to have an upper bound $L_{i,max}$ for queue length $l_i(t)$. In applications, $L_{i,max}$ can be decided by the critical queue length that may cause spillback on approach i. Therefore, the state constraints are:

$$0 \le l_i(t) \le L_{i,max}, \forall i = 1, 2, 3, 4. \tag{2.2}$$

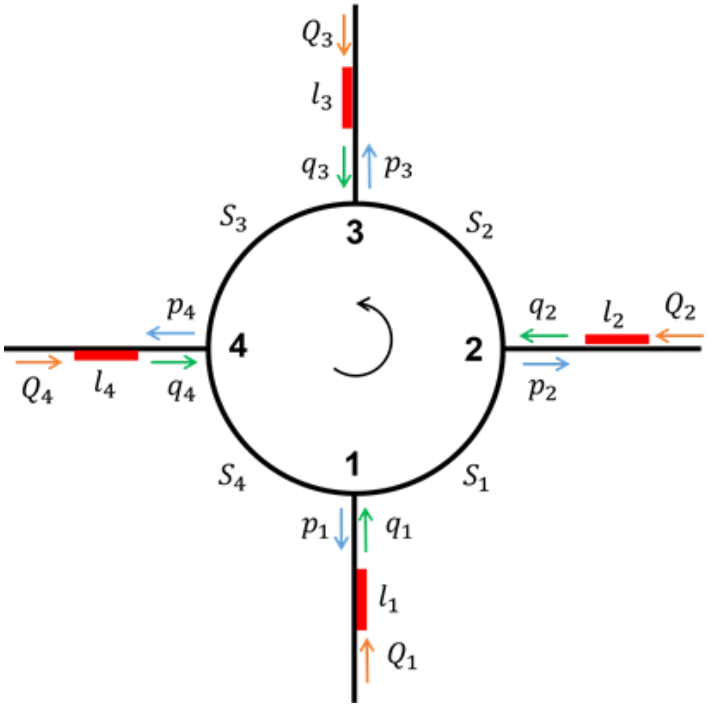

Figure 2.1: Four-approach roundabout

To model the constraints of control inputs q_i, the roundabout segments are introduced and described. As seen in Fig 2.1, the circular roundabout is separated by four approaches into four arc-shaped segments, S_1, S_2, S_3, and S_4. Since these segments are likely to have similar road design as they belong to the same roundabout, it is assumed that all segments have the same service capacity $Q_{S,max}$ (i.e., the upper bound of segment flow q_{S_k}, $k = 1, 2, 3, 4$). Note that q_{S_k} may consist of vehicles from every approach. For example, vehicles entering from approach 1 heading to approach 3 will drive through S_1 and S_2, and thereby contribute to both q_{S_1} and q_{S_2}. Similarly, vehicles entering from approach 2 heading to approach 1 will also drive through S_2, thereby contributing to q_{S_2}. Denote flows from approach i heading to approach j as q_{ij} $(i, j = 1, 2, 3, 4)$, which can be represented as $q_{ij} = \eta_{ij} q_i$, where η_{ij} is the proportion of the flow heading to approach j in the merge-in flow from approach i. To describe the relationships between S_k and q_{ij}, define the service tables of four segments as follows (note that this study assumes that vehicles will drive through each segment no more than once when passing through the roundabout). The element in row i and column j of the service table for S_k, a_{ij}^k, is an indicator variable of whether q_{ij} will pass through S_k. For instance, $a_{22}^4 = 1$, indicating the U-turn flow from approach 2 will pass through S_4 in the roundabout; while $a_{32}^2 = 0$ means vehicles coming from approach 3 heading to approach 2 will not drive through S_2. Therefore, the flow on S_k is:

$$q_{S_k}(t) = \sum_{i=1}^{4} \sum_{j=1}^{4} a_{ij}^k \eta_{ij} q_i(t), \forall k = 1, 2, 3, 4 \tag{2.3}$$

Then, the control input constraints can be represented as

$$q_{S_k}(t) \leq Q_{S,max}, \forall k = 1, 2, 3, 4 \tag{2.4}$$

$$q_i(t) > 0, \forall i = 1, 2, 3, 4 \tag{2.5}$$

The control objective is

$$\min_{q_1, q_2, q_3, q_4} \int_0^{\Delta\tau} \left(\sum_{i=1}^{4} \frac{Q_i l_i(t)}{q_i(t)} \right) dt \tag{2.6}$$

where $l_i(t)/q_i(t)$ is the estimated waiting time for vehicles at the end of the queue on approach i, and $Q_i dt$ is the number of incoming vehicles or vehicles joining the queue at the end on approach i. Therefore, the integration can be interpreted as the total estimated waiting time of vehicles arriving from $t = 0$ to $t = \Delta\tau$. Compared to the vehicle-level delay representation, Eq. (2.6) provides an informative and computationally tractable estimation for the total system delay. The complexity of the problem does not increase with the number of vehicles, enabling its use in real-time applications. The optimal control problem defined by Eq. (2.1)~(2.6) falls in the domain of nonlinear optimal control, which generally does not have analytical solutions. Therefore, a direct collection method (Beiner & Paris 1987) is applied to solve it, which converts the optimal control problem into a

nonlinear optimization problem by discretizing state variables $l_i(t)$ and control inputs $q_i(t)$ into vectors $\hat{\boldsymbol{l}}_{\boldsymbol{i}} = [l_i(0), \dots, l_i(\Delta\tau)], \hat{\boldsymbol{q}}_{\boldsymbol{i}} = [q_i(0), \dots, q_i(\Delta\tau)]$.

2.2 Vehicle merge-in decision control

Given the optimal merge-in flows from the last subsection, the intersection controller needs to coordinate vehicles coming from four approaches on when they should merge to achieve the desired merge-in flows. Therefore, a probabilistic merge-in decision control model is developed to determine when the vehicles at the head of queues can start to merge in. In this way, the flow-level control inputs are converted into an optimal vehicle passing sequence, which can be connected to vehicle-level operations.

Let the spare capacity s_k of each segment k denote the difference between the capacity $Q_{S,max}$ and the flow on S_k, that is $s_k(t) = Q_{S,max} - q_{S_k}(t)$. Define S_1, S_2, S_3, and S_4 as the upstream segment of approaches $2, 3, 4$, and 1, respectively. Apart from the spare capacity from approach i's upstream segment, there is additional p_i capacity available for vehicles on approach i, which can be described as follows:

$$p_i(t) = \sum_{j=1}^{4} \eta_{ji} q_j(t), \forall i = 1, 2, 3, 4, \tag{2.7}$$

Note that p_i can also be interpreted as the flow that diverges out at approach i (diverge-out flow). Therefore, the total available capacity for the merge-in flow of approach i (suppose its upstream segment is S_k) is $s_k + p_i$. Let P_i denote the probability of the leading vehicle on approach i choosing to merge into the circular flow within the roundabout whenever there is available capacity. Then, the probability P_i should satisfy the following condition to achieve the desired merge-in flows:

$$P_i = \frac{q_i}{Q_{S,max} - q_{S_k} + p_i} \tag{2.8}$$

where S_k is the upstream segment of approach i. With this condition met, the actual merge-in flow from approach i would be $P_i(s_k + p_i) = q_i$. Following Eq. (2.3) and (2.7), it is proved that $0 < P_i \leq 1$, which guarantees that our decision control is applicable at all times.

2.3 Vehicle platoon control

Assume the specific information packet of interest belongs to an arbitrary information class j, $j \in \mathcal{L}$. This section seeks to model the information dissemination wave in the upper layer under the designed queuing strategy. It describes the instantaneous change in the density (veh/km) of equipped vehicles by vehicle class (i.e., S, H, R, E for information packets in class j) due to V2V communications. The impacts of communication constraints (communication power, communication frequency, signal interference, etc.) on the success of V2V communications is explicitly factored in this model.

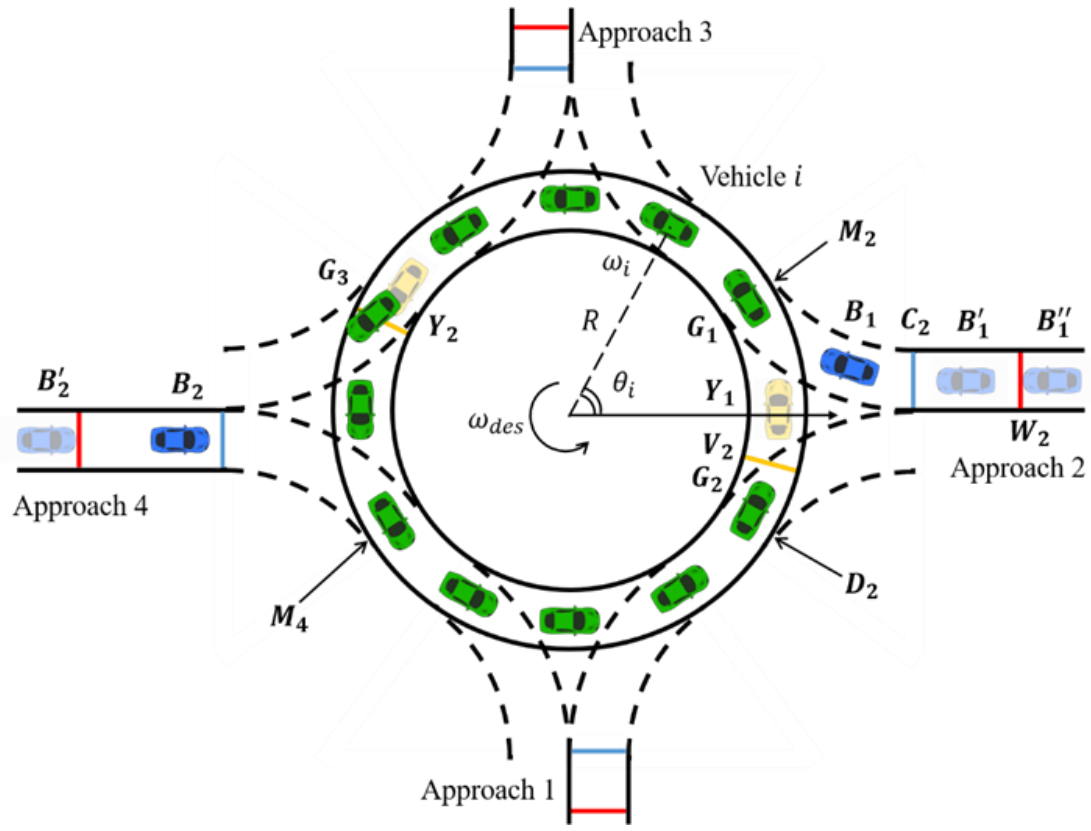

Figure 2.2: Illustration of self-adjusting stage and virtual platoon control stage in vehicles' merge-in procedure

Once vehicles choose to merge into the roundabout based on the probabilistic decision control model, they will start the merge-in procedure and eventually cruise with the circular platoon until they diverge to the approaches they are heading to. The merge-in procedure consists of a self-adjusting stage and a virtual platoon control stage. Figure 2.2 illustrates an example of the two stages using the merge-in procedure of vehicle B_1. First, B_1 waits at position W_2 (marked by a red line) when it is at the head of the queue on approach 2. When the decision control model allows it to merge into a spare slot (labeled the matching slot of B_1) in the platoon, B_1 enters the self-adjusting stage. The objective of this stage is to have vehicle B_1 drive through a critical position C_2 (marked by a blue line on approach 2) to enter the virtual platoon control stage at the desired speed v_{des} after some desired time Δt_{des}. The desired speed is also the desired cruising speed of the platoon.

The desired time Δt_{des} is estimated as the time it takes for the matching slot to travel to a virtual critical position V_2 (marked by the yellow line on the right part of the roundabout in Figure 2.2) from the beginning of the self-adjusting stage. The virtual critical position

V_2 is a projection of C_2 on the roundabout circle, that is $|M_2V_2| = |M_2C_2|$, where M_2 is a merging point of the roundabout and the on-ramp from approach 2. When vehicle B_1 travels from C_2 to M_2, a virtual vehicle Y_1, which is the projection of B_1, also travels from V_2 to M_2. At the same time, B_1 communicates with vehicles G_1 and G_2, making Y_1 behave like a vehicle communicating with its surrounding vehicles in the circular platoon. This stage is labeled as the virtual platoon control stage. Note that when determining the length of $|M_2C_2|$, $|M_2D_2| \geq |M_2C_2| = |M_2V_2|$ should be ensured, where D_2 is the diverging point of the off-ramp to approach 2. It is assumed that once a diverging vehicle passes the diverging point and drives to the off-ramp, it is no longer a part of the circular platoon (i.e., its movement will not affect surrounding vehicles in the platoon anymore). This guarantees that during the virtual platoon control stage, there will be no real diverging vehicle at the slot where the virtual vehicle projected from a real merge-in vehicle is located. Otherwise, they may have a conflicting influence on the surrounding vehicles since they are at the same slot in the platoon.

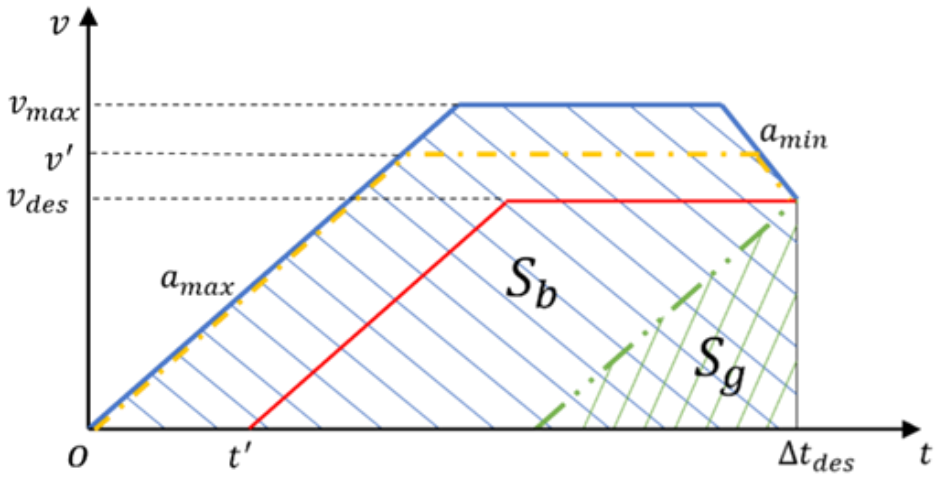

Figure 2.3: Feasible speed trajectories for vehicles in the self-adjusting stage

The control of a vehicle from approach i in the self-adjusting stage can be formulated as:

$$\int_0^{\Delta t_{des}} v(t)dt = |C_iW_i| \tag{2.9.1}$$

$$v(\Delta t_{des}) = v_{des} \tag{2.9.2}$$

$$0 \leq v(t) \leq v_{max}, \forall t \in [0, \Delta t_{des}] \tag{2.9.3}$$

$$a_{min} \leq \frac{dv(t)}{dt} \leq a_{max}, \forall t \in [0, \Delta t_{des}] \quad (2.9.4)$$

where $v_{max}, a_{min}, a_{max}$ are the maximum speed, maximum deceleration, and maximum acceleration, respectively. As shown in Figure 2.3, in a speed-time graph, the formulation seeks for trajectories starting from (0,0) ending at $(\Delta t_{des}, v_{des})$, whose time integration equals to $|C_i W_i|$. The formulation can have multiple feasible solutions if $S_g \leq |C_i W_i| \leq S_b$, where S_g and S_b are the blue (right)-shaded and green (left)-shaded areas, respectively, in Figure 2.3. One feasible strategy is to follow the speed trajectory indicated by the yellow (dash-dot)/red (dash-dot-dot) lines when $|C_i W_i|$ is greater than or equal to/less than $\frac{v_{des}^2}{2a_{max}} + v_{des}(\Delta t_{des} - \frac{v_{des}}{a_{max}})$.

The merge-in procedure will be seamless if the transition of two stages is as precise as described in the literature. However, it is possible that when the matching slot arrives at the virtual critical position, the vehicle is not exactly at the critical position at the desired speed because a critical parameter Δt_{des} is estimated and possibly inaccurate when solving**Error! Reference source not found.**). For example, in Figure 2.2, the matching slot of vehicle B_2 arrives at the diverging point with the diverging vehicle G_3 earlier than Δt_{des}. Also, it is possible that, at Δt_{des}, G_3 still needs a little more time to get to the off-ramp. Then, B_2 will have passed the critical point when G_3 leaves the platoon. Note that the start time of the virtual platoon control stage is when the available slot arrives at the diverging point, not when the vehicle arrives at the critical point or the blue lines in Figure 2.2. Therefore, the virtual platoon control should ensure stability to mitigate the initial speed and position errors introduced by virtual vehicles when they enter the virtual platoon control stage.

To ensure stability, the circular platoon in the roundabout is investigated, which consists of real vehicles, virtual vehicles projected from the vehicles on on-ramps at the second merge-in stage, and some spare vehicle slots. Note that here we assume a circular roundabout for simplicity; however, the model is not restricted only to ideal circular roundabouts. The platoon control model can be extended to non-circular roundabouts by mapping the roadways to circular roundabouts with the same road length. Suppose that when the roundabout serves at its maximum capacity, there are N homogeneous vehicles cruising in the roundabout with a desired angular speed $\omega_{des} = v_{des}/R$ (where R is the radius of the roundabout). It implies that the roundabout has N vehicle slots labeled from 1 to N. When there are spare vehicle slots, the circular platoon can be converted into one (if there is only one spare vehicle slot) or more linear vehicle platoons using the spare slots to separate them. Then, existing linear CACC platoon control strategies (Wang, Wu & Barth 2018) can be applied.

For a circular platoon with no spare vehicle slots, a symmetric bidirectional control architecture is developed (where predecessor and follower position errors influence the vehicle controller symmetrically). As shown in Figure 2.2, an angular coordinate θ_n, ω_n is used to describe the position and angular speed of vehicle n (i.e., vehicle matched with

vehicle slot n). Each vehicle is modeled as a double integrator. The control inputs for vehicle n in the platoon are assumed to depend only on its speed error $\omega_n - \omega_{des}$ and the relative headway errors between itself and its immediate neighbors (i.e., its predecessor and follower). Denote the positions of the preceding and following vehicles of vehicle n as θ_n^p and θ_n^f, respectively. The desired angular headway is $\Delta = 2\pi/N$. The vehicle dynamics can be described as:

$$\frac{d\theta_n(t)}{dt} = \omega_n \tag{2.10.1}$$

$$\frac{d\omega_n(t)}{dt} = -k_v(\omega_n - \omega_{des}) + k_d\left(\theta_n^p - \theta_n - \Delta\right) - k_d\left(\theta_n - \theta_n^f - \Delta\right) \tag{2.10.2}$$

where k_v and k_d are positive constants. To facilitate analysis, a coordinate change is considered using the initial position of slot 1, $\theta_1(0)$, as a reference point:

$$\tilde{\theta}_n(t) = \theta_n(t) - \omega_{des}t - \theta_1(0) - (n-1)\Delta \tag{2.11.1}$$

$$\tilde{\omega}_n(t) = \omega_n(t) - \omega_{des} \tag{2.11.2}$$

To describe the dynamics of the circular platoon, define $\tilde{\boldsymbol{\theta}} \coloneqq \left[\tilde{\theta}_1, \tilde{\theta}_2, \dots, \tilde{\theta}_N\right]^T$, $\tilde{\boldsymbol{\omega}} \coloneqq [\tilde{\omega}_1, \tilde{\omega}_2, \dots, \tilde{\omega}_N]^T$. Substituting Eq. (2.11) into Eq. (2.10), the following is obtained:

$$\begin{bmatrix}\dot{\tilde{\boldsymbol{\theta}}} \\ \dot{\tilde{\boldsymbol{\omega}}}\end{bmatrix} = \begin{bmatrix}\mathbf{0} & \boldsymbol{I} \\ -k_d\boldsymbol{T} & -k_v\boldsymbol{I}\end{bmatrix}\begin{bmatrix}\tilde{\boldsymbol{\theta}} \\ \tilde{\boldsymbol{\omega}}\end{bmatrix}, \tag{2.12}$$

where

$$\boldsymbol{T} = \begin{bmatrix} 2 & -1 & 0 & \dots & 0 & -1 \\ -1 & 2 & -1 & 0 & \dots & 0 \\ 0 & -1 & 2 & -1 & \cdots & 0 \\ \vdots & \ddots & \ddots & \ddots & \ddots & \vdots \\ 0 & \dots & 0 & -1 & 2 & -1 \\ -1 & 0 & \dots & 0 & -1 & 2 \end{bmatrix}. \tag{2.13}$$

Eq. (2.12) indicates that the circular platoon to be controlled is a linear system. The following lemma (Philip 1979) illustrates the non-negativity of $\boldsymbol{T}$'s eigenvalues.

Lemma 1 . *Given an $n \times n$ circulant matrix $\boldsymbol{C}$ with the form*

$$\boldsymbol{C} = \begin{bmatrix} c_0 & c_{n-1} & \dots & c_2 & c_1 \\ c_1 & c_0 & c_{n-1} & \dots & c_2 \\ \vdots & c_1 & c_0 & \ddots & \vdots \\ c_{n-2} & \dots & \ddots & \ddots & c_{n-1} \\ c_{n-1} & c_{n-2} & \dots & c_1 & c_0 \end{bmatrix} \tag{2.14}$$

the normalized eigenvectors are the Fourier modes, namely,

$$v_j = \frac{1}{\sqrt{n}}\left(1, \kappa^j, \kappa^{2j}, \dots, \kappa^{(n-1)j}\right), j = 0, 1, \dots, n-1, \tag{2.15}$$

where $\kappa = \exp\left(\frac{2\pi i}{n}\right)$ *and* i *is the imaginary unit. The corresponding eigenvalues are:*

$$\lambda_j = c_0 + c_{n-1}\kappa^j + c_{n-2}\kappa^{2j} + \cdots + c_1\kappa^{(n-1)j}, j = 0, 1, \dots, n-1 \tag{2.16}$$

Note that $\boldsymbol{T}$ is a $N \times N$ circulant matrix with $c_0 = 2, c_1 = c_{N-1} = -1, c_i = 0$ $(i = 2, 3, \dots, N-2)$. According to Lemma 1, the j^{th} eigenvalue of $\boldsymbol{T}$ is

$$\lambda_{Tj} = 2 - \kappa^j - \kappa^{(N-1)j}, j = 0, 1, \dots, N-1, \tag{2.17}$$

where $\kappa = \exp\left(\frac{2\pi i}{N}\right)$. Note that $\kappa^{(N-1)j} = -\kappa^j$. Therefore,

$$\lambda_{Tj} = 2 - \kappa^j - \kappa^{-j} = 2 - 2\cos\left(\frac{2\pi j}{N}\right) \geq 0, j = 0, 1, \dots, N-1, \tag{2.18}$$

Theorem 1 . *The equilibrium states for a general linear time-invariant system* $\dot{x} = Ax$ *are stable if and only if each eigenvalue* λ_A *of A satisfies* $\Re(\lambda_A) \leq 0$ *and* $\Re(\lambda_A) < 0$ *if* λ_A *is defective, where* $\Re(\lambda_A)$ *is the real part of* λ_A.

From Theorem 1 (Theorem 5.4 of (Johan Åström & Murray 2010)), the eigenvalues of the system can be described by Eq. (2.12) as follows:

$$\begin{bmatrix} \boldsymbol{0} & \boldsymbol{I} \\ -k_d\boldsymbol{T} & -k_v\boldsymbol{I} \end{bmatrix}\begin{bmatrix} \tilde{\boldsymbol{\theta}} \\ \tilde{\boldsymbol{\omega}} \end{bmatrix} = \lambda\begin{bmatrix} \tilde{\boldsymbol{\theta}} \\ \tilde{\boldsymbol{\omega}} \end{bmatrix}$$
$$(\lambda^2 + k_v\lambda)\tilde{\boldsymbol{\theta}} = -k_d\boldsymbol{T}\tilde{\boldsymbol{\theta}} \tag{2.19}$$

With $\boldsymbol{T}$'s eigenvalues $\lambda_{Tj}, j = 0, 1, \dots, N-1$, we have

$$\lambda^2 + k_v\lambda + k_d\lambda_{Tj} = 0$$
$$\lambda = \frac{-k_v \pm \sqrt{k_v^2 - 4k_d\lambda_{Tj}}}{2} \tag{2.20}$$

Recall that Eq. (2.18) has shown the non-negativity of λ_{Tj}. Therefore, for $k_v, k_d > 0$, $\Re(\lambda) \leq 0$ and when $k_v^2 - 4k_d\lambda_T = 0$, $\Re(\lambda) = -k_v/2 < 0$. According to Theorem 1, the equilibrium states of Eq. (2.12) are stable.

3. NUMERICAL STUDIES

To demonstrate the performance of the proposed CAV control strategy at roundabouts, several numerical studies are conducted for a four-approach single-lane roundabout with $N = 12$ vehicle slots. The desired speed v_{des} is set as 8 m/s (17.9 mph). The service capacity of the roundabout $Q_{S,max}$ is 60 vehicles/minute. The control time period $\Delta\tau = 5$ minutes. Note that in real-world applications, the control time period is related to the variation of incoming flows. The principle for the determination of $\Delta\tau$ is that the incoming flows do not change significantly within the control time period because the optimal merge-in flows are solved based on the constant incoming flow assumption.

First, the effectiveness of the roundabout flow control is investigated. The parameters and initial conditions for each approach are shown in Table 3.1.

Figure 3.1 shows the optimal control trajectory of merge-in flows, queue lengths, and segment flows of the system. Five phases (separated by dashed lines) are observed in the 5-minute optimal control solution. Within each phase, the control inputs (merge-in flows) remain constant, and the queue lengths change linearly. Figure 3.1(c) shows that the maximum capacity constraints for the four segments are all active in the first phase, indicating that the roundabout is operating at its maximum capacity. Each time a queue disappears, the system adjusts the merge-in flows, which demonstrates the adaptiveness of the control strategy.

The number of active segment-maximum-capacity constraints decreases with the number of non-zero queues. Because when there is no queue on approach i, the corresponding merge-in flow $q_i = Q_i$. With fewer undetermined control inputs, fewer constraints are active. In the last phase, when there is no queue on four approaches, the merge-in flow q_i on each approach is equal to the incoming flow Q_i. Compared to conventional roundabouts' first-come-first-serve principle, the cooperation among the four approaches is also reflected in the results. For example, the queue on approach 2 grows in the first phase to prioritize vehicles from other approaches with higher demand pressures (i.e., longer queues or higher incoming flows). However, in real-world applications, some approaches may have an upper bound on queue length to avoid spillbacks.

Figure 3.2 illustrates how the queue lengths evolve with/without an upper-bound value of three, on the length of queue on approach 2, l_2. Figure 3.2(b) illustrates that after l_2 reaches 3, the system prioritizes vehicles from the other approaches. However, it adjusts the merge-in flows to meet the queue length constraint on approach 2.

Table 3.1: Experiment settings

Approach ID (i)	1	2	3	4
Q_i (vehicles/minute)	30	25	35	20
$l_i(0)$	2	1	3	4

For $\boldsymbol{\eta} = [\eta_{ij}]$, the experiment uses the following setting:

$$\boldsymbol{\eta} = \begin{bmatrix} 0.0 & 0.7 & 0.2 & 0.1 \\ 0.2 & 0.0 & 0.6 & 0.2 \\ 0.8 & 0.1 & 0.0 & 0.1 \\ 0.1 & 0.5 & 0.4 & 0.0 \end{bmatrix}. \tag{3.1}$$

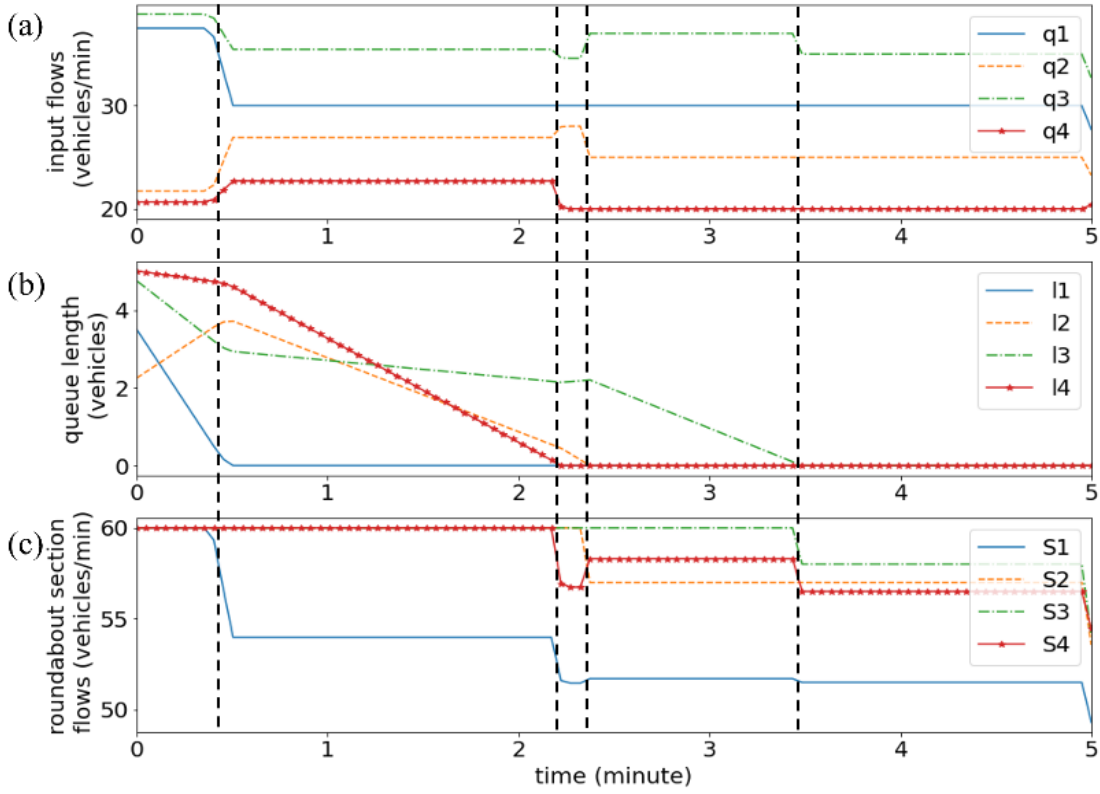

Figure 3.1: Optimal merge-in flows, queue lengths, and segment flows

Figure 3.1 shows the optimal control trajectory of merge-in flows, queue lengths, and segment flows of the system. Five phases (separated by dashed lines) are observed in the 5-minute optimal control solution. Within each phase, the control inputs (merge-in flows) remain constant, and the queue lengths change linearly. Figure 3.1(c) shows that the maximum capacity constraints for the four segments are all active in the first phase, indicating that the roundabout is operating at its maximum capacity. Each time a queue disappears, the system adjusts the merge-in flows, which demonstrates the adaptiveness of the control strategy.

The number of active segment-maximum-capacity constraints decreases with the number of non-zero queues. Because when there is no queue on approach i, the corresponding merge-in flow $q_i = Q_i$. With fewer undetermined control inputs, fewer constraints are active. In the last phase, when there is no queue on four approaches, the merge-in flow q_i on each approach is equal to the incoming flow Q_i. Compared to conventional roundabouts' first-come-first-serve principle, the cooperation among the four approaches is also reflected in the results. For example, the queue on approach 2 grows in the first phase to prioritize vehicles from other approaches with higher demand pressures (i.e., longer queues or higher incoming flows). However, in real-world applications, some approaches may have an upper bound on queue length to avoid spillbacks.

Figure 3.2 illustrates how the queue lengths evolve with/without an upper-bound value of three, on the length of queue on approach 2, l_2. Figure 3.2(b) illustrates that after l_2 reaches 3, the system prioritizes vehicles from the other approaches. However, it adjusts the merge-in flows to meet the queue length constraint on approach 2.

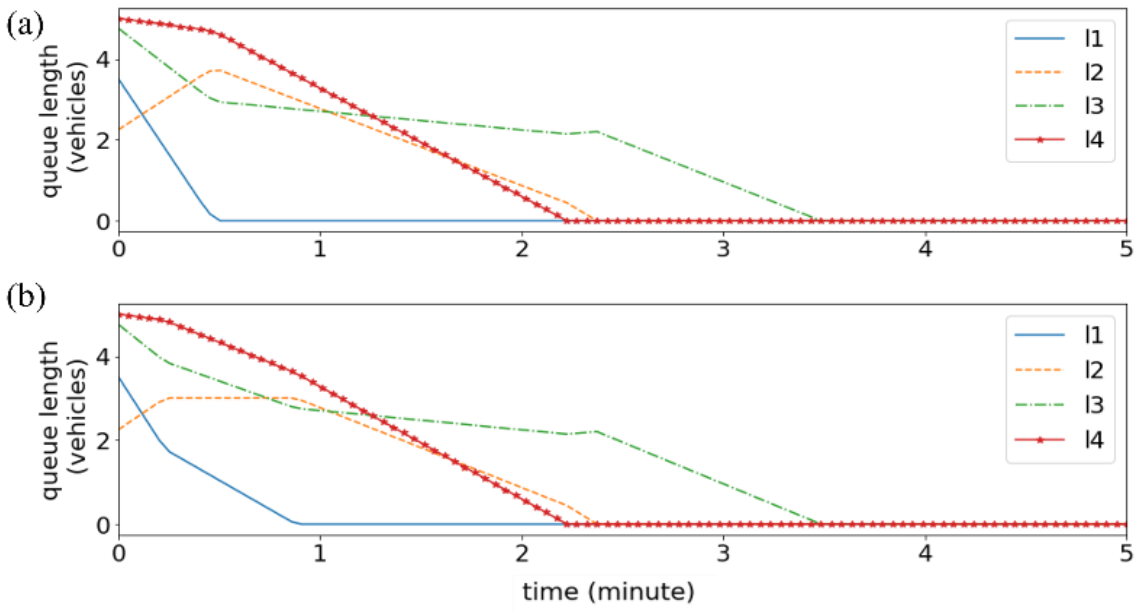

Fig. 3.2: Queue length evolution: (a) without and (b) with queue length upper bound

Next, the stability performance of the circular platoon control is validated. Note that the merge-in control and the self-adjusting stage are not simulated. It is assumed that the occurrence of merging-in follows a Poisson distribution ($\lambda = 1$), and the initial speed and position disturbances follow a uniform distribution $[-1, 1]$ m/s and a uniform distribution $[-1, 1]$ m, respectively. Figure 3.3 shows the position errors, headways, and speed errors of 12 vehicles due to disturbances introduced by newly merging vehicles. The equilibrium state of the circular platoon changes each time a new vehicle merges in. For example, in Figure 3.3(a), vehicles' equilibrium states in the platoon move in the same circular direction (counterclockwise in Figure 2.2) during $t = 30{\sim}46$ seconds because of continuous positive position errors introduced by new merge-in vehicles. However, it is related more to coordinate shifts and does not influence vehicle safety. Figure 3.3(b) shows that vehicles' headways remain in a safe range (the desired time headway is set as 1 second) during the entire simulation. Figure 3.3(c) illustrates that all newly introduced speed errors can be mitigated in a short time. The spikes in Figures 3.3(b) and 3.3(c) mostly occur on on-ramps because position and speed errors are introduced by virtual vehicles. It allows the system to converge closer to the equilibrium state before real vehicles merge into the circular platoon, which enhances smoothness and safety.

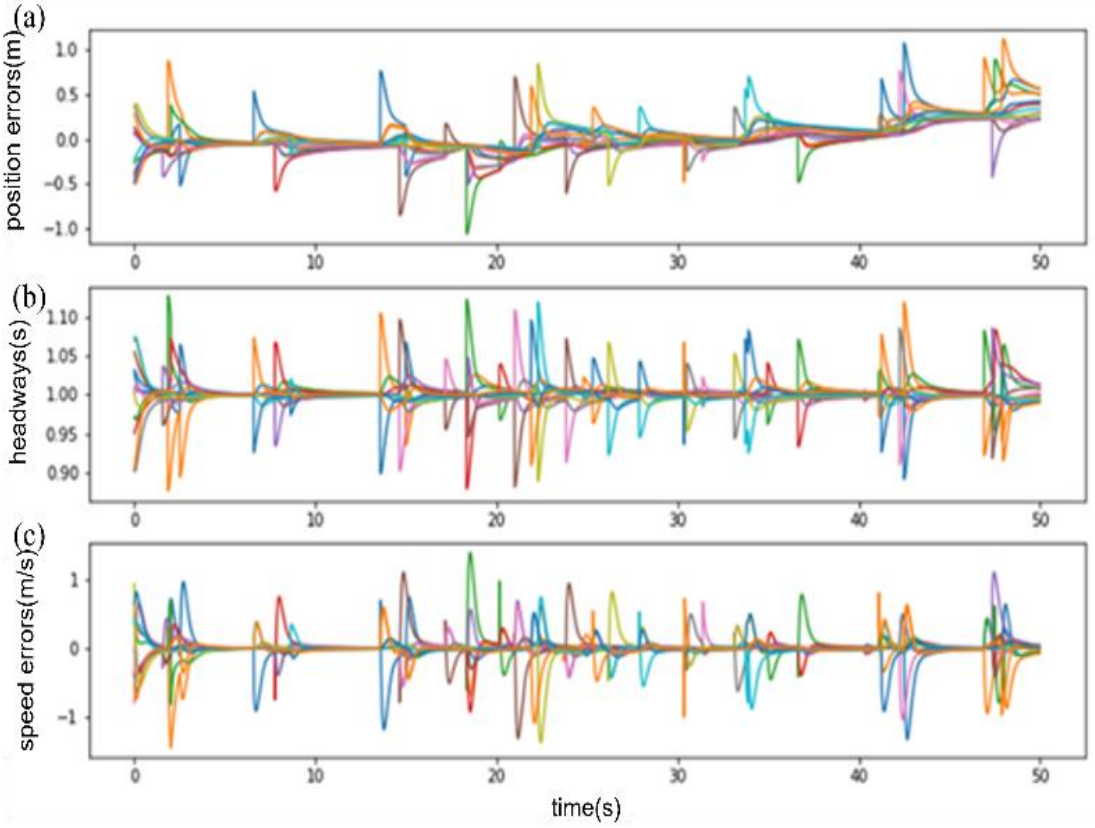

Figure 3.3: Stability and safety analysis of virtual platoon control

In summary, the performances of both upper-level flow control and lower-level vehicle control are illustrated separately. Next, these two components are integrated with the proposed vehicle merge-in control and a comprehensive simulation is performed. Note that in flow-level control, the vehicle-level randomness in the incoming flow is neglected. Also, the vehicle merge-in control assumes instantaneous changes of within-roundabout flow due to merge-in flows. Hence, the overall performance of the proposed model can be less efficient than the performance determined from the roundabout flow control component. In the following comparison, the idealized performance associated with the roundabout flow control is used as a benchmark.

Table 3.2: Demand settings for performance comparison

Intersection design	East and West Bound		North and South Bound	
	Through demand (veh/h/lane)	Left-turn demand (veh/h/lane)	Through demand (veh/h/lane)	Left-turn demand (veh/h/lane)
Two-lane roundabout	1125	450	1125	450
Four-lane crossroad	1500	600	1500	600

To compare the overall performance of the proposed roundabout control strategy with other intersection control strategies, the demand pattern associated with the high demand case (case 6) in Mirheli et al. (2019) is used. Table 3.2 shows that though the demands are different, the proportions of corresponding demands in the two intersection designs are identical (0.75). As the roundabout model uses only a two-lane roadway setting, it is not meaningful to compare its performance using the demand on various approaches of typical four-lane crossroads. To address this issue, and account for the effects of different time headway settings and different numbers of lanes on incoming approaches, a new intersection design efficiency measure labeled as i is proposed, which is the throughput of the intersection divided by the sum of the capacity of all input lanes. The intersection design efficiency quantifies the capability of the intersection design (both flow pattern design and control strategy design) to serve the capacity of all incoming approaches. The proposed unit-free measure is justified as follows. The most efficient intersection design is to use separate facilities (for example, grade-separated roads) to connect all approaches. Thereby, vehicles traveling in different directions will not affect each other, which implies that the intersection can serve the capacity of all incoming approaches (regardless of the number of lanes and how large the capacities are); thus $i = 1$. This "perfect" intersection design serves as an idealized benchmark to evaluate the efficiency of various intersection designs using i.

Table 3.3: Performance comparison

Intersection design	East and West Bound		North and South Bound	
	Through demand (veh/h/lane)	Left-turn demand (veh/h/lane)	Through demand (veh/h/lane)	Left-turn demand (veh/h/lane)
Two-lane roundabout	1125	450	1125	450
Four-lane crossroad	1500	600	1500	600

The proposed measure enables comparisons between intersection designs with different incoming approach capacities. The results for signal-free intersection control, fully actuated signal control, and fixed-time signal control are from Mirheli et al. (2019) (simulated on intersections with four-lane roads). The proposed roundabout control strategy is simulated for an intersection with two-lane roads (one lane in each direction). The seven-minute (including a two-minute warm-up) simulation recording can be accessed online[1]. As shown by Table 3.3, while the signal-free intersection control strategy from Mirheli et al. (2019) has the highest throughput, its intersection design efficiency is only 0.188. This is because the "cross" flow pattern in conventional intersection design has significant conflicts associated with the flows from different directions, which limits the spatiotemporal occupancy within the intersection. By leveraging CAVs, the roundabouts' circular flow pattern can fully exploit road capacity inside the intersection. The overall performance of the proposed roundabout control yields a high intersection design efficiency, 0.343, which is almost twice that of the signal-free intersection control strategy. Also, note that the intersection design efficiency calculated from flow-level control is higher than that of the overall control, indicating that the proposed model suffers mild efficiency loss when converting optimal merge-in flows into vehicle-level controls. This is because the upper-level flow control neglects the vehicle level randomness. However, solving optimal control problems at the flow level mitigates the computational burden compared to signal-free intersection control in Mirheli et al. (2019) which directly solves the high-dimensional vehicle-level optimal control problem.

Figure 3.4 shows a screenshot of the simulation recording, which illustrates the integration of the proposed control components. The blue dots are incoming vehicles and platooning vehicles, while the orange ones are vehicles that have passed through the roundabout. In the top-right zoomed-in view, desired positions of platooning vehicles (slot positions) are marked with the slot number labeled. The bottom-right of Figure 3.4 shows that the speed errors and headway errors of the platooning vehicles in the last 250 steps (the step size is 0.05 seconds) are updated dynamically. Damping patterns can be observed similar to those in the validation of the platoon stability in Figure 3.3. The top-left part of the figure shows that the queue length on approaches 1, 2, and 3 are 1, 2, 1, respectively. Interestingly, an analysis of the roundabout flow control components indicates that there should be no queues during the entire time period. However, due to vehicle-level randomness, the queue lengths in the comprehensive simulation have positive values all the

[1] https://youtu.be/XEZhPJnr4eg

time, leading to different intersection design efficiencies, 0.343 and 0.438 for the entire model and the flow control model, respectively, as shown in Table 3.3.

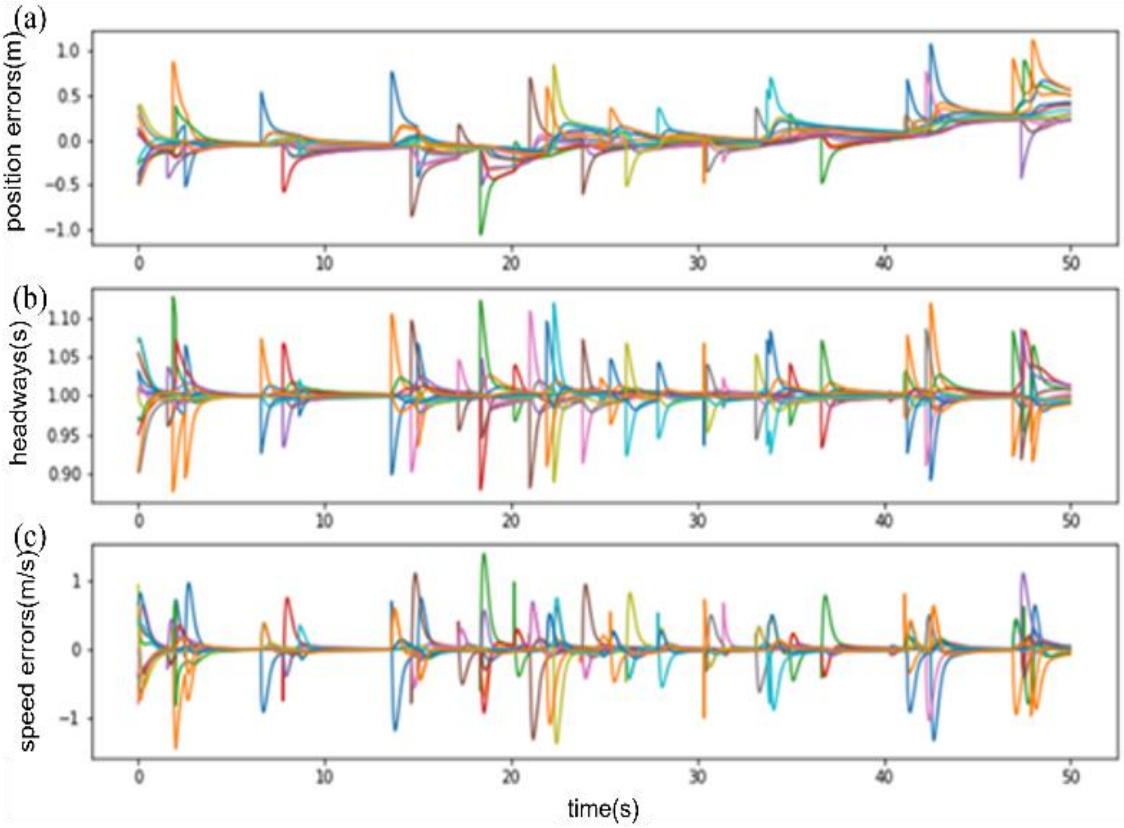

Figure 3.4: Simulation of the proposed roundabout control strategy

4. FINDINGS AND CONCLUSIONS

This study aims to fill a gap in the current literature by illustrating the advantages of roundabouts in a CAV environment. The main contributions of this study are to: (i) develop a hierarchical roundabout control framework to decouple system performance measures and vehicle safety constraints, to relieve the computational burden by significantly decreasing the dimension of the optimal control problem; (ii) investigate the potential advantages of roundabout designs compared to traditional intersection designs to provide insights for future infrastructure design in urban networks in CAV environments; and (iii) extend existing linear CACC models to a circular CACC virtual platoon control model to address the safety and stability considerations for vehicles operating within a roundabout.

5. RECOMMENDATIONS

This study suggests another potential venue for intersection infrastructure design for CAVs beyond signal-free intersections. The study insights provide directions for further research, including: (i) leveraging closed-loop control strategies such as model predictive control to enhance the roundabout flow control performance; (ii) extending the proposed control strategy to multilane roundabouts; and (iii) investigating roundabout control problem in a mixed traffic environment.

6. SYNOPSIS OF PERFORMANCE INDICATORS

6.1 Part I

The research carried out in this study can be described as advanced research. The research was presented at the 2019 INFORMS Annual Meeting at Seattle, WA, and the Transportation Research Board 2022 Annual Meeting in Washington, DC. This project supported 1 student at the doctoral level.

6.2 Part II

Two (2) conference articles and one (1) peer-reviewed journal articles were produced from this project. The outputs, outcomes, and impacts are described in Section 7 below.

7. OUTPUTS, OUTCOMES, AND IMPACTS

7.1 Outputs

Journal paper

- Wang, C., Wang, Y., Peeta, S. (2022). Cooperative Roundabout Control Strategy for Connected and Autonomous Vehicles. *Applied Science*, 12(24), 12678; https://doi.org/10.3390/app122412678.

Conferences

- Wang, C., Wang, Y., Peeta, S. (2019). Cooperative Roundabout Control Strategy for Connected and Autonomous Vehicles. Annual Meeting of Institute for Operations Research and the Management Sciences (INFORMS), Seattle, WA, USA.

- Wang, C., Wang, Y., Peeta, S. (2022). Cooperative Roundabout Control Strategy for Connected and Autonomous Vehicles. 101st Annual Meeting of Transportation Research Board (TRB), Washington, D.C, USA.

7.2 Outcomes

Rigorous mathematical models are developed to explore the effectiveness of the circular flow pattern at intersections. Specifically, this research develops a hierarchical roundabout control framework to decouple system performance measures and vehicle safety constraints, to relieve the computational burden by significantly decreasing the dimension of the optimal control problem. The potential advantages of roundabout designs compared to traditional intersection designs are investigated to provide insights for future infrastructure design in urban networks in CAV environments. In addition, existing linear CACC models to a circular CACC virtual platoon control model is extended to address the safety and stability considerations for vehicles operating within a roundabout. The results of this study demonstrates that (i) the roundabout flow control can coordinate the merging

flows from different directions to enhance the efficiency; (ii) the vehicle platoon control can dampen the oscillations induced by the speed and positional errors at the self-adjusting stage to ensure vehicle safety; (iii) the merge-in control is able to integrate the aforementioned two components with slight impairment to the solution optimality; and (iv) the proposed roundabout control strategy shows the advantage of the circular flow pattern over the "cross" flow pattern in terms of the intersection design efficiency.

7.3 Impacts

The findings of this study provide valuable insights on future traffic operations and infrastructure design at intersections. The roundabout control model provides the traffic manager/operator a hierarchical framework to develop effective intersection control solutions following the circular flow pattern instead of the "cross" flow pattern. The insights can assist decision-makers to design effective planning and operational strategies that promote the benefits of CAVs and enhance traffic performance at intersections under mixed traffic flows during the transition to a fully autonomous and connected transportation system.

7.4 Tech Transfer

In the execution of this project (titled Adapting Land Use and Infrastructure for Automated Driving), the research team undertook a number of technology transfer activities. First, the research team published one articles in technical journals with a wide readership, high reputation, and high impact factor. The team also gave presentations at the 2019 INFORMS annual meeting with total conference attendance exceeding 6,000 and the TRB annual meeting, a conference with over 14,000 attendees. Further, a number of tech transfer activities were undertaken as part of this project, such as communication with other universities through webinars and forums. The list below summarizes the tech transfer activities undertaken by the research team through the course of this project:

In 2019:
1. Conference presentation at the Annual Meeting of Institute for Operations Research and the Management Sciences (INFORMS), Seattle, W.A, USA: Cooperative Roundabout Control Strategy for Connected and Autonomous Vehicles, by Wang, C., Wang, Y., & Peeta, S.

In 2022:
1. Technical paper in Applied Science: Cooperative Roundabout Control Strategy for Connected and Autonomous Vehicles, by Wang, C., Wang, Y., & Peeta, S.
2. Conference presentation at the 101st Annual Meeting of Transportation Research Board (TRB), Washington, D.C, USA: Cooperative Roundabout Control Strategy for Connected and Autonomous Vehicles, by Wang, C., Wang, Y., & Peeta, S.

8. REFERENCES

Banjanovic-Mehmedovic, L., Halilovic, E., Bosankic, I., Kantardzic, M. & Kasapovic, S., 2016, 'Autonomous Vehicle-to-Vehicle (V2V) Decision Making in Roundabout using Game Theory', International Journal of Advanced Computer Science and Applications, 7(8).

Beiner, L. & Paris, S.W., 1987, 'Direct trajectory optimization using nonlinear programming and collocation', Journal of Guidance, Control, and Dynamics, 10(4).

Eisenman, S., Josselyn, J., List, G., Persaud, B., Lyon, C., Robinson, B., Blogg, M., Waltman, E. & Troutbeck, R.J., 2004, Operational and Safety Performance of Modern Roundabouts and Other Intersection Types, vol. 37.

Eom, M. & Kim, B.I., 2020, The traffic signal control problem for intersections: a review, European Transport Research Review, 12(1).

González, D., Pérez, J. & Milanés, V., 2017, 'Parametric-based path generation for automated vehicles at roundabouts', Expert Systems with Applications, 71.

Johan Åström, K. & Murray, R.M., 2010, Feedback systems: An introduction for scientists and engineers.

Levin, M.W. & Rey, D., 2017, 'Conflict-point formulation of intersection control for autonomous vehicles', Transportation Research Part C: Emerging Technologies, 85.

Li, Z., Elefteriadou, L. & Ranka, S., 2014, 'Signal control optimization for automated vehicles at isolated signalized intersections', Transportation Research Part C: Emerging Technologies, 49.

Malikopoulos, A.A., Cassandras, C.G. & Zhang, Y.J., 2018, 'A decentralized energy-optimal control framework for connected automated vehicles at signal-free intersections', Automatica, 93.

Mirheli, A., Tajalli, M., Hajibabai, L. & Hajbabaie, A., 2019, 'A consensus-based distributed trajectory control in a signal-free intersection', Transportation Research Part C: Emerging Technologies, 100.

Nie, J., Zhang, J., Ding, W., Wan, X., Chen, X. & Ran, B., 2016, 'Decentralized Cooperative Lane-Changing Decision-Making for Connected Autonomous Vehicles∗', IEEE Access, 4.

Philip, D., 1979, Circulant Matrices, Wiley, New York, NY.

Rastelli, J.P. & Peñas, M.S., 2015, 'Fuzzy logic steering control of autonomous vehicles inside roundabouts', Applied Soft Computing Journal, 35.

Retting, R.A., Mandavilli, S., McCartt, A.T. & Russell, E.R., 2006, 'Roundabouts, traffic flow and public opinion', Traffic Engineering and Control, 47(7).

Tian, R., Li, S., Li, N., Kolmanovsky, I., Girard, A. & Yildiz, Y., 2018, Adaptive Game-Theoretic Decision Making for Autonomous Vehicle Control at Roundabouts, Proceedings of the IEEE Conference on Decision and Control, vols 2018-December.

Wang, C., Gong, S., Zhou, A., Li, T. & Peeta, S., 2020, 'Cooperative adaptive cruise control for connected autonomous vehicles by factoring communication-related constraints', Transportation Research Part C: Emerging Technologies, 113.

Wang, Z., Wu, G. & Barth, M.J., 2018, A Review on Cooperative Adaptive Cruise Control (CACC) Systems: Architectures, Controls, and Applications, IEEE Conference on Intelligent Transportation Systems, Proceedings, ITSC, vols 2018-November.

APPENDIX

CCAT Project: Adapting Land Use and Infrastructure for Automated Driving

Paper 1: Wang C, Wang Y, Peeta S. Cooperative Roundabout Control Strategy for Connected and Autonomous Vehicles. *Applied Sciences*. 2022; 12(24):12678. https://doi.org/10.3390/app12241267

Intersections in the urban network are potential sources of traffic flow inefficiency. Existing intersection control mostly adopts the "cross" flow pattern model, while the use of the roundabout circular flow pattern is rather sparse. Connected and autonomous vehicle (CAV) technologies can enable roundabouts to better compete with traditional intersection designs in terms of performance. This study proposes a roundabout control strategy for CAVs to enhance intersection performance while ensuring vehicle safety. A hierarchical framework is developed to decouple the flow-level performance objective and vehicle-level safety constraints to achieve computational tractability for real-time applications. It entails developing a roundabout flow control model to optimize merge-in flows, a merge-in decision model to generate vehicle passing sequence from the optimal flows, and a virtual platoon control model to achieve safe and stable vehicle operations in a circular roundabout platoon. The performance of the proposed roundabout control strategy is illustrated through numerical studies and compared to existing intersection control methods. Its stability and safety characteristics are also demonstrated.